



**CHALMERS**  
UNIVERSITY OF TECHNOLOGY

## **A Click Chemistry-Based Artificial Metallo-Nuclease**

Downloaded from: <https://research.chalmers.se>, 2026-04-05 04:36 UTC

Citation for the original published paper (version of record):

Gibney, A., de Paiva, R., Singh, V. et al (2023). A Click Chemistry-Based Artificial Metallo-Nuclease. *Angewandte Chemie - International Edition*, 62(38).  
<http://dx.doi.org/10.1002/anie.202305759>

N.B. When citing this work, cite the original published paper.



# A Click Chemistry-Based Artificial Metallo-Nuclease

Alex Gibney, Raphael E. F. de Paiva, Vandana Singh, Robert Fox, Damien Thompson, Joseph Hennessy, Creina Slator, Christine J. McKenzie, Pegah Johansson, Vickie McKee, Fredrik Westerlund, and Andrew Kellett\*

**Abstract:** Artificial metallo-nucleases (AMNs) are promising DNA damaging drug candidates. Here, we demonstrate how the 1,2,3-triazole linker produced by the Cu-catalysed azide-alkyne cycloaddition (CuAAC) reaction can be directed to build Cu-binding AMN scaffolds. We selected biologically inert reaction partners *tris*(azidomethyl)mesitylene and ethynyl-thiophene to develop TC-Thio, a bioactive C<sub>3</sub>-symmetric ligand in which three thiophene-triazole moieties are positioned around a central mesitylene core. The ligand was characterised by X-ray crystallography and forms multinuclear Cu<sup>II</sup> and Cu<sup>I</sup> complexes identified by mass spectrometry and rationalised by density functional theory (DFT). Upon Cu coordination, Cu<sup>II</sup>-TC-Thio becomes a potent DNA binding and cleaving agent. Mechanistic studies reveal DNA recognition occurs exclusively at the minor groove with subsequent oxidative damage promoted through a superoxide- and peroxide-dependent pathway. Single molecule imaging of DNA isolated from peripheral blood mononuclear cells shows that the complex has comparable activity to the clinical drug temozolomide, causing DNA damage that is recognised by a combination of base excision repair (BER) enzymes.

## Introduction

Nucleic acids are essential to life on earth, with the remarkable stability of the phosphodiester backbone providing the integrity required for faithful storage of genetic information.<sup>[1]</sup> Artificial metallo-nucleases (AMNs) are small molecules capable of cleaving nucleic acids, resulting in either loss of genetic integrity or overactivation of DNA damage repair mechanisms and ultimately apoptosis.<sup>[2]</sup> Therefore, AMNs are promising candidates in the search for new metallodrugs and here we report a click chemistry method for preparing a new polynuclear Cu-binding AMN that we call Cu<sup>II</sup>-TC-Thio. AMNs can be classified as either hydrolytic or oxidative cleavage agents. Hydrolytic AMNs mimic the activity of natural restriction enzymes and catalyse the direct cleavage of the phosphodiester backbone, resulting in hydroxylated and phosphorylated ends that can typically be repaired by ligases.<sup>[3]</sup> Oxidative AMNs catalyse strand cleavage through redox processes such as H-atom abstraction from the deoxyribose ring, causing a radical cascade that forms more complex lesions requiring sophisticated and energetically expensive repair processes.<sup>[4]</sup> Extensive research efforts have been devoted to the investigation of Cu<sup>II</sup> AMNs, with modification to both the ligand structure and coordination environment, conferring modulated reactivity at the DNA interface.<sup>[5]</sup>

There is now significant interest in developing polynuclear Cu<sup>II</sup> AMNs due to their potent activity—often referred to as ‘self-’ or ‘unattended-’ activation—stemming from cooperative reactivity pathways that do not require

[\*] A. Gibney, Dr. R. E. F. de Paiva, R. Fox, Dr. J. Hennessy, Dr. C. Slator, Prof. Dr. V. McKee, Prof. Dr. A. Kellett  
 SSPC, the Science Foundation Ireland Research Centre for Pharmaceuticals, School of Chemical Sciences, Dublin City University  
 Glasnevin, Dublin 9, Dublin (Ireland)  
 E-mail: andrew.kellett@dcu.ie  
 Dr. V. Singh, Prof. Dr. F. Westerlund  
 Department of Life Sciences, Chalmers University of Technology  
 Gothenburg (Sweden)  
 Dr. V. Singh  
 Department of Biological Engineering, Massachusetts Institute of Technology  
 Cambridge, MA (USA)  
 Prof. Dr. D. Thompson  
 SSPC, the Science Foundation Ireland Research Centre for Pharmaceuticals, Department of Physics, University of Limerick  
 (Ireland)

Prof. Dr. C. J. McKenzie, Prof. Dr. V. McKee  
 Department of Physics, Chemistry and Pharmacy, University of Southern Denmark  
 Campusvej 55, 5230 Odense M (Denmark)

Dr. P. Johansson  
 Laboratory of Clinical Chemistry, Sahlgrenska University Hospital  
 Gothenburg  
 (Sweden)  
 and  
 Department of Laboratory Medicine, Institute of Biomedicine,  
 Sahlgrenska Academy at University of Gothenburg  
 (Sweden)

© 2023 The Authors. Angewandte Chemie International Edition published by Wiley-VCH GmbH. This is an open access article under the terms of the Creative Commons Attribution License, which permits use, distribution and reproduction in any medium, provided the original work is properly cited.

reagents such as ascorbate or peroxide.<sup>[6]</sup> The triazole linker generated in the Cu-catalysed alkyne-azide cycloaddition (CuAAC) reaction can coordinate metal ions<sup>[7]</sup> and tag macromolecules with coordinating pockets.<sup>[8]</sup> We recently reported a synthetic strategy to ‘click’ a series of simple amines to a *tris*(azidomethyl)mesitylene (triazide) core.<sup>[9]</sup> One of the resulting Tri-Click (TC) ligands, TC-1 (Figure S1), was found to chelate Cu<sup>II</sup> ions and displayed AMN activity. Here, we present TC-Thio, a Tri-Click scaffold containing three discrete triazole-thiophene planar groups designed—according to the HSAB (hard and soft (Lewis acids and bases) principle—to coordinate Cu<sup>II</sup> and Cu<sup>I</sup> redox pairs and provide enhanced DNA binding properties (Figure 1).

## Results and Discussion

### Preparation of TC-Thio and its Cu<sup>II</sup> binding properties

The preparation of TC-Thio began with the azidation of 1,3,5-tris(bromomethyl)-2,4,6-trimethylbenzene, and the subsequent CuAAC reaction of this triazide with three equivalents of 2-ethynylthiophene generated the desired product. While optimising the reaction, screening of various conditions found that pre-activating a *tris*(3-hydroxypropyltriazolylmethyl)amine (THPTA)-Cu<sup>II</sup> co-catalyst with sodium-*L*-ascorbate produced higher yields with greater purity than experiments where the components were

added separately, or which lacked THPTA (Supplementary 1.2 and Figure S2–S6). The conditions efficiently promoted ‘click chemistry’ as TC-Thio was isolated in high yield (84 %) from aerobic reaction conditions using polar solvents that required a simple (non-chromatographic) work up (Figure S2–S6). Single crystals were subsequently obtained by slow evaporation of a solution of TC-Thio in DCM/MeOH/ACN (2:1:1). Single crystal structure analysis confirmed the tripodal structure of the TC-Thio molecule (Figures 2a, S7 and S8).<sup>[10]</sup> Details of the structure analysis are included in section S1.3 and Table S1. Electrospray ionization mass spectrometry (ESI-MS) analysis of a 50:50 DMF:water solution containing TC-Thio and three molar equivalents of Cu<sup>II</sup> nitrate trihydrate showed the presence of tri-, di- and mononuclear species that could be preliminarily identified by their isotopic distribution patterns. For all three species, the mono-cationic form—generated from the loss of a single nitrate—was found, with [Cu(TC-Thio)-(NO<sub>3</sub>)]<sup>+</sup> at 734.07 m/z, [Cu<sub>2</sub>(TC-Thio)(NO<sub>3</sub>)<sub>2</sub>]<sup>+</sup> at 920.98 m/z and [Cu<sub>3</sub>(TC-Thio)(DMF)(NO<sub>3</sub>)<sub>3</sub>]<sup>+</sup> at 1180.94 m/z (Figure 2b). For simplicity, solutions containing TC-Thio and three equivalents of Cu<sup>II</sup> nitrate, which likely contain a mixture of free ligand in addition to the mono-, di- and trinuclear complexes, are henceforth referred to as Cu<sup>II</sup>-TC-Thio. Thiophenes are generally poor donors to most transition metal ions but can undergo a variety of reactions in organometallic and coordination compounds<sup>[11]</sup> including with soft metal ions such as Cu<sup>I</sup>.<sup>[12]</sup> Therefore, while triazole-thiophene groups are most likely to bind to Cu<sup>II</sup> primarily via the nitrogen donor, possibly supported by weak coordination to the sulfur, sulfur-binding should be enhanced on reduction of Cu<sup>II</sup> to Cu<sup>I</sup> (*cf.* crystal structures in Figure S9b). To provide insight into the structure of Cu<sup>II</sup>-TC-Thio, we conducted density functional theory (DFT) calculations (supplementary S1.5). As a first step calculations using a molecular model of the TC-Thio ligand as the input structure were performed (Figure S9a) as a starting point to calculate a structure for the trinuclear Cu<sup>II</sup>-TC-Thio complex. The calculated electronic structure of the trinuclear Cu<sup>II</sup>-TC-Thio complex showed each Cu atom coordinated to TC-Thio in a monodentate fashion through a triazole nitrogen donor (N3) and to possess square pyramidal geometry (Figure 2c). The coordination sphere is completed by a water molecule and two nitrate anions; all but one of the nitrate ions make a strong bond to the Cu<sup>II</sup> ion in the square plane and a longer interaction via a second oxygen donor. The model retains the conformation of the free ligand, with two triazole-thiophene groups on one side of the mesitylene plane and one on the other. The latter site contains a Cu<sup>II</sup> ion bound with one purely monodentate nitrate and there is a plausible interaction of the sulfur donor as a weak apical ligand in square pyramidal geometry (Cu–S 3.42 Å). The hypothesis that Cu<sup>I</sup> can bind more strongly with the thiophene sulfur donor is supported by crystallographic data for several related complexes (Figure S9b). In iodo-bis[2-(thiophen-2-yl)-4,5-dihydro-1H-imidazole]-Cu<sup>I</sup> the metal ion is 5-coordinate but the Cu–S distances are long (> 2.9 Å).<sup>[12a]</sup> In the second example, [2-(1-benzothiophen-2-yl)-pyridine],[bis(triphenylphosphane)]-

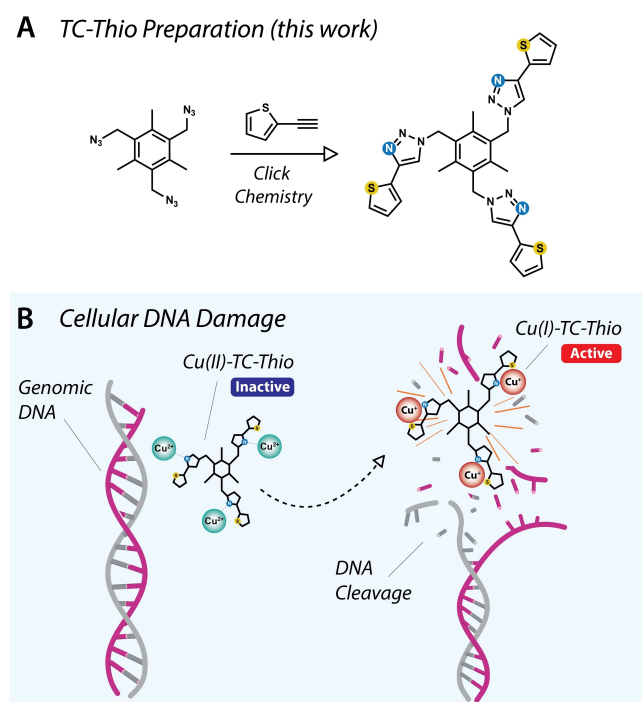


**Figure 1.** A. Synthesis of TC-Thio using Cu<sup>I</sup>-catalysed click chemistry. B. TC-Thio coordinates three Cu<sup>II</sup> ions predominantly through N-triazole coordination. Upon reduction, the S-thiophenyl becomes non-innocent to enable Cu<sup>I</sup> chelation and potent oxidative DNA damage.

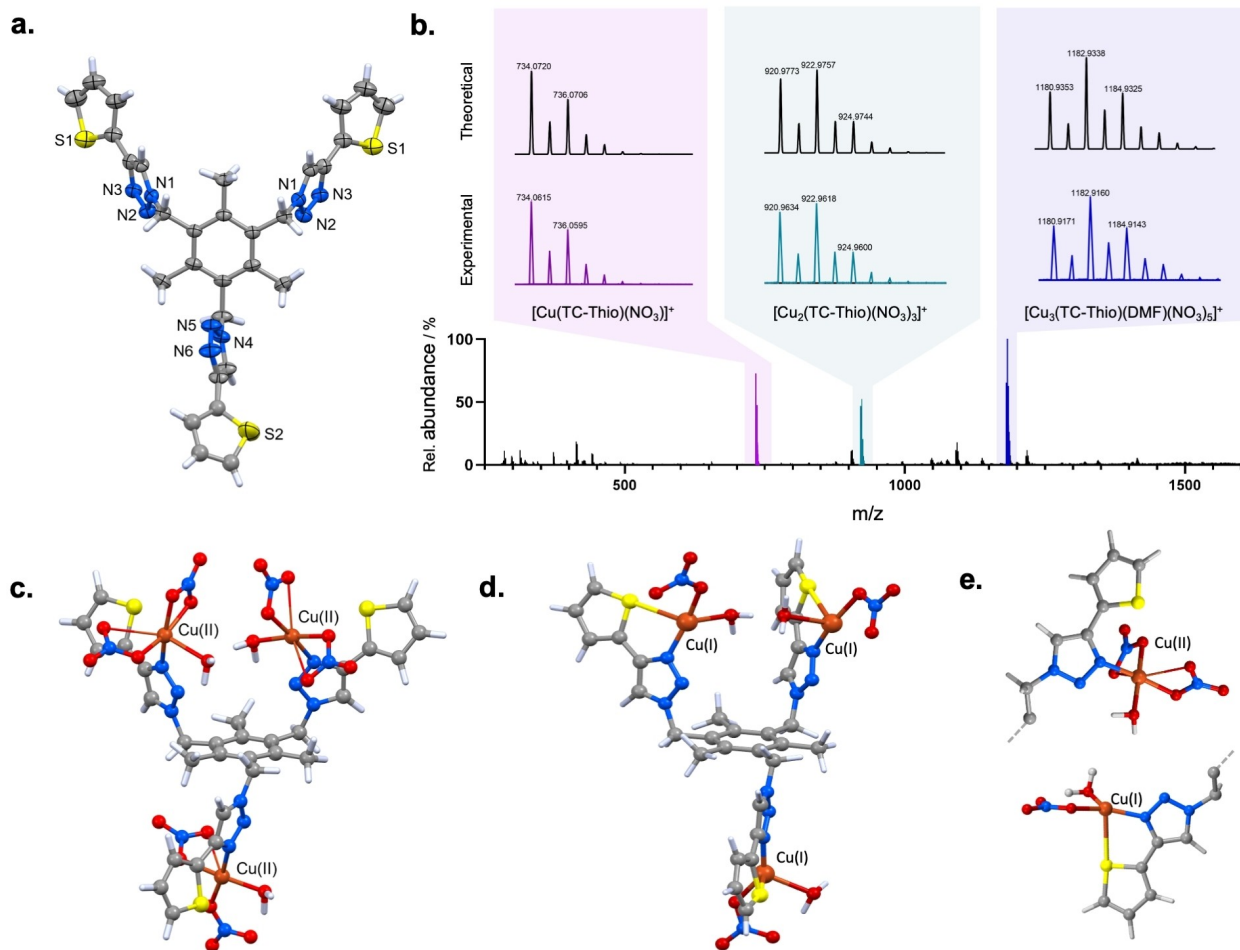


**Figure 2.** a. Molecular structure of TC-Thio showing 30% probability ellipsoids and omitting disorder. b. ESI-MS spectrum of TC-Thio in the presence of three molar equivalents of  $\text{Cu}(\text{NO}_3)_2 \cdot 3\text{H}_2\text{O}$  carried out in 1:1 DMF/water. The spectrum (bottom) reveals identifiable species:  $[\text{Cu}(\text{TC-Thio})(\text{NO}_3)]^+$ ,  $[\text{Cu}_2(\text{TC-Thio})(\text{NO}_3)_3]^+$  and  $[\text{Cu}_3(\text{TC-Thio})(\text{NO}_3)_5(\text{DMF})]^+$  in purple, green and blue, respectively. Theoretical (black) and experimental isotope patterns are in excellent agreement. c. DFT computed complex of TC-Thio with three equivalents of  $\text{Cu}^{\text{II}}$  nitrate and coordinated water molecules. d. DFT computed alternative complex of TC-Thio with three equivalents of  $\text{Cu}^{\text{I}}$  nitrate and coordinated water molecules. e. selected coordination spheres of  $\text{Cu}^{\text{II}}$  (top) and  $\text{Cu}^{\text{I}}$  (bottom) extracted from part c. and d., respectively.

$\text{Cu}^{\text{I}}$  tetrafluoroborate,<sup>[12b]</sup> the geometry is a somewhat flattened tetrahedron and the Cu–S distance is 2.69 Å. The DFT calculations for  $\text{Cu}^{\text{I}}$ -TC-Thio reported here (Figure 2d) resulted in generally distorted tetrahedral Cu geometries with Cu–S distances of 2.9 Å predicting N,S chelation involving non-innocent S-thiophenyl coordination with  $\text{Cu}^{\text{I}}$ .

### $\text{Cu}^{\text{II}}$ -TC-Thio DNA binding interactions

The DNA binding properties of  $\text{Cu}^{\text{II}}$ -TC-Thio were investigated using a range of direct and indirect techniques including fluorescence quenching, fluorescence melting, circular dichroism, and microscale thermophoresis. First, fluorescent displacement experiments using calf thymus DNA (ctDNA) pre-saturated with ethidium bromide (EtBr) were examined.<sup>[13]</sup> TC-Thio displays  $\text{Cu}^{\text{II}}$ -dependent DNA binding with the 3:1  $\text{Cu}^{\text{II}}$ -TC-Thio complex having an apparent DNA binding constant ( $K_{\text{app}}$ ) of  $1.1 \times 10^7 \text{ M}^{-1}$

(Figure 3a). These results indicate  $\text{Cu}^{\text{II}}$ -TC-Thio is a high affinity  $\text{Cu}^{\text{II}}$  DNA binding agent.<sup>[6c,14]</sup> Significantly, no appreciable quenching activity of EtBr was observed in the presence of TC-Thio ligand alone. Next, to identify the potential binding site interaction, fluorescence quenching experiments were carried out with Hoechst 34580—a minor groove binder—and methyl green (MG)—a major groove binder (Figure 3b).  $\text{Cu}^{\text{II}}$ -TC-Thio efficiently quenched Hoechst 34580 ( $Q_{\text{Hoechst}} = 14.41 \mu\text{M}$ ), while only limited quenching of MG was detected ( $Q_{\text{MG}} \gg 100 \mu\text{M}$ ) indicating that the complex selectively binds in the minor groove. To explore the DNA binding properties further, a series of Dickerson–Drew hairpins (DDHs) dodecamers containing short adenine loops were designed to enable direct analysis through circular dichroism, microscale thermophoresis, and fluorescence melting experiments (Figure S10). The first hairpin developed (FRET-DDH) contained the FRET pair 5'-Alexa Fluor 647 and 3'-Iowa Black (Q) and was designed for fluorescence melting. The second hairpin (DDH) was

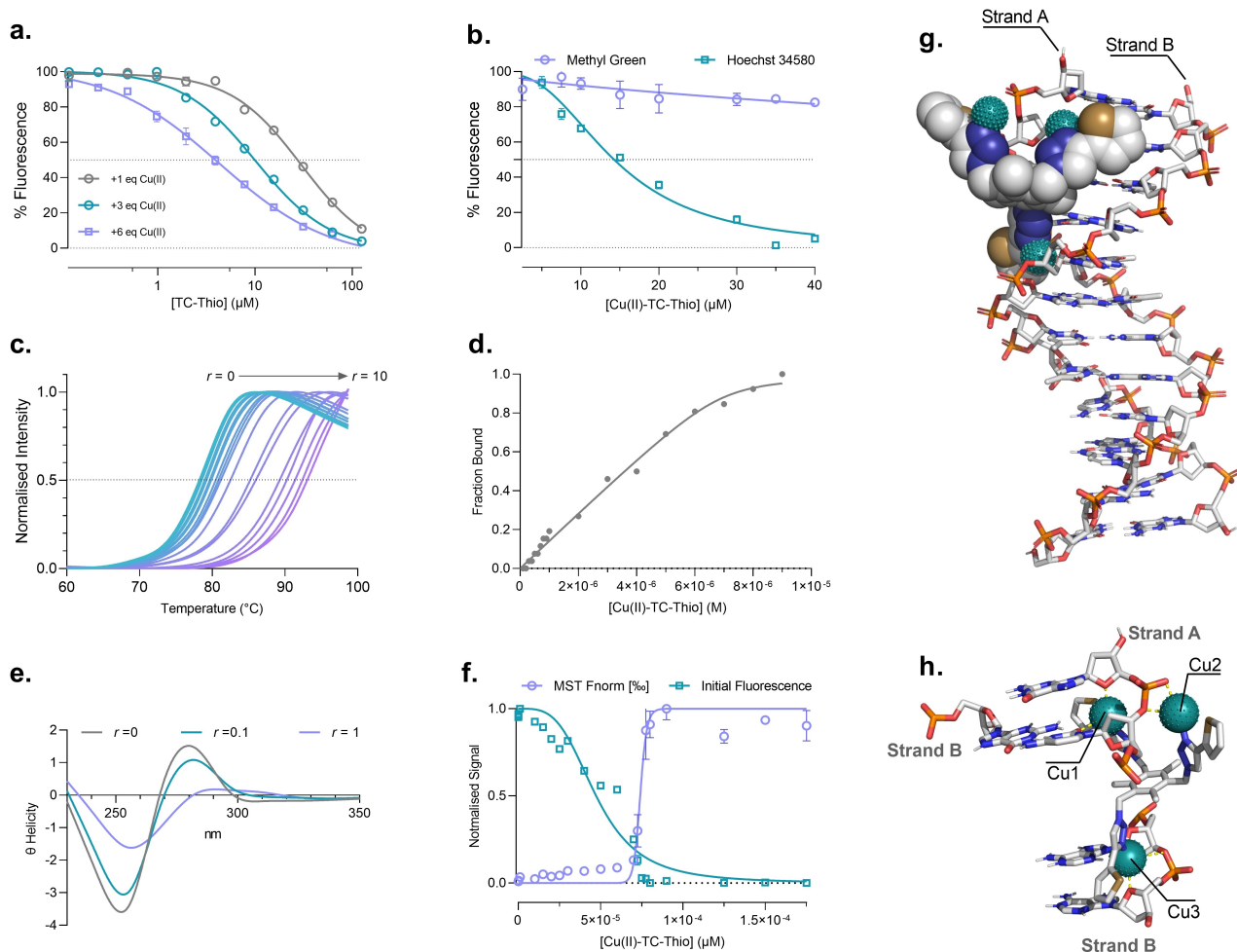


**Figure 3.** a. Displacement of EtBr from ctDNA by TC-Thio in the presence of 2 and 3 equivalents of  $\text{Cu}^{\text{II}}$  nitrate (the graph of 3 equivalents was used to calculate  $K_{\text{app}} = 1.1 \times 10^7 \text{ Mbp}^{-1}$ ). b. Competitive displacement of minor groove binder Hoechst 34580 and major groove binder methyl green from ctDNA. c. Fluorescence melting of FRET-DDH with increasing  $\text{Cu}^{\text{II}}$ -TC-Thio loading,  $T_m$  is taken as the midpoint of the normalised melting curve. d. Fitting of Bard equation with the fluorescence melting data obtained in c. e. CD analysis of DDH in the presence of 0.0, 0.1 and 1.0 equivalents of  $\text{Cu}^{\text{II}}$ -TC-Thio. f. Normalised data and initial intensity data obtained from microscale thermophoresis experiments conducted with F-DDH. g. Best-ranked pose of docking simulations conducted using the Dickerson–Drew dodecamer (PDB: 1BNA) as the receptor and  $\text{Cu}^{\text{II}}$ -TC-Thio (in space-filling representation) as the ligand. h. Detail of the binding region of  $\text{Cu}^{\text{II}}$ -(TC-Thio), highlighting the polar contacts of Cu atoms, shown as yellow dashed lines. All error bars shown represent standard error of the mean from triplicate values.

unlabelled and designed for use in circular dichroism (CD) analysis, and the third hairpin (F-DDH) contained a 5'-Alexa fluor 647 (F) modification for use in microscale thermophoresis (MST) analysis. Fluorescence melting analysis was monitored in the absence and presence of  $\text{Cu}^{\text{II}}$ -TC-Thio ( $r=0-10$  where  $r=[\text{complex}]/[\text{DNA}]$ ). The native FRET-DDH sequence recorded a  $T_m$  of  $79^\circ\text{C}$  which increased dose-dependently on addition of the  $\text{Cu}^{\text{II}}$ -TC-Thio complex (Figure 3c). The fraction of bound complex to FRET-DDH ( $\alpha$ ) was then calculated ( $\alpha = \Delta T_m / \Delta T_{\text{max}}$ ) and plotted against  $\text{Cu}^{\text{II}}$ -TC-Thio concentration (Figure 3d). The resulting plot was then fit to the Bard equation<sup>[15]</sup> ( $R^2 = 0.99$ ) which returned a  $K_b = 5.8 \times 10^7 \text{ M}^{-1}$  and an occupancy of 3.5 molecules per hairpin. The  $K_b$  value is in excellent agreement with the earlier  $K_{\text{app}}$  value obtained through EtBr fluorescence quenching. CD experiments with the second hairpin, DDH, revealed a decrease in intensity at 250 and

280 nm when  $\text{Cu}^{\text{II}}$ -TC-Thio binds, corresponding to a loss of helicity and base pair  $\pi-\pi$  stacking interactions, respectively (Figure 3e). The CD data support a non-intercalative binding mode consistent with minor groove recognition,<sup>[6c]</sup> and the significant loss in helicity (observed at  $r=1.0$ ) may also indicate condensation effects. To probe this potential interaction further, MST experiments—a relatively new technique that quantifies molecular interactions based on changes in thermophoretic mobility—were conducted (Figure 3f).<sup>[16]</sup> Analysis of the  $\%F_{\text{Norm}}$  signal, typically used in MST analysis, revealed an  $\text{EC}_{50}$  value of  $\sim 70 \mu\text{M}$  ( $\approx 1400 \text{ eq.}$ ) which, given the earlier calculated  $K_{\text{app}}$  and  $K_b$  values, suggests a signal change due to condensation of the F-DDH hairpin. To confirm this interaction, we analysed the initial fluorescence signal and found a dose-dependent decrease. While this condensation behaviour may, to some extent, be expected for a trinuclear transition metal com-

plex, this is the first observation that Cu<sup>II</sup>-TC-Thio shares similarities with DNA condensing C<sub>3</sub>-symmetric opioid-based agents.<sup>[17]</sup> Finally, to help confirm the nature of the Cu<sup>II</sup>-TC-Thio DNA binding mode, preassociative molecular docking studies with the Dickerson–Drew dodecamer (DDD; PDB code: 1BNA) were undertaken. Here, 1BNA was treated as a rigid oligomer and the starting position of the complex was randomised to minimise starting position bias (see Supporting Information S1.10 for full details). Docking results suggest that binding of Cu<sup>II</sup>-TC-Thio to the DDD occurs exclusively within the minor groove (Figure 3g and 3 h) with none of the top ten most stable poses showing major groove residency. For simplicity, the strands of 1BNA were labelled A and B while the relative location of Cu centres on the duplex were measured in base pairs from the top of Figure 3g, with the first base pair referred to as bp1. Cu1 resides within the minor groove between bp1 and bp2 in this motif, and binds to a carbonyl group of a cytosine base (2.6 Å) and the endocyclic oxygen atom of the neighbouring nucleotide (2.3 Å) on strand A. Cu2 is docked external to the groove and coordinates phosphate (2.5 Å) and the bridging oxygen (2.6 Å) between bp1 and bp2, also on strand A, in similar fashion to that observed for other multinuclear transition metal complexes.<sup>[6c]</sup> Cu3 is located within the minor groove between the bp5 and bp6 and reveals endocyclic oxygen coordination (2.4 Å), similar to that observed for Cu1 and a longer interaction with the bridging phosphate oxygen (3.5 Å) similar to Cu2, with both interactions occurring with strand B. Overall, these inter-strand interactions in free, uncomplexed DNA would be expected to induce significant thermal stabilization by acting as a molecular bridge between the two DNA strands and to initiate condensation via backbone neutralisation.

### Cu<sup>II</sup>-TC-Thio mediates DNA oxidative damage

The artificial metallonuclease (AMN) activity of Cu<sup>II</sup>-TC-Thio was investigated using an agarose-based DNA cleavage assay. Here, supercoiled pUC19 plasmid was incubated with varying concentrations of the complex and the conversion of supercoiled to open circular or linear DNA via single and double strand breaks were monitored by gel electrophoresis and band densitometry. Typically, such experiments are run in the presence of a reductant such as sodium-*L*-ascorbate which generates the redox active Cu<sup>I</sup> oxidation state and primes the complex for DNA cleavage. There is significant interest however in self-activated agents that can induce DNA damage in the absence of reductant. Examples of these self-activated AMNs include bis-phenanthroline Cu<sup>II</sup> phthalate complexes<sup>[5b]</sup> and natural products such as colibactins—a series of human gut genotoxins, for which Cu is a vital cofactor.<sup>[6a]</sup> We conducted initial DNA cleavage experiments in the absence of reductant and found that samples which contained Cu<sup>II</sup>-TC-Thio presented significantly more degradation than samples of equivalent Cu<sup>II</sup> concentrations alone (Figure S11a). Experiments conducted in the presence of Na-*L*-ascorbate showed the gradual conversion of supercoiled to open circular and eventual appearance of linear

DNA with well-defined dose responses (Figure 4a, s11b and S11c). Data here suggest the preclusion of independent double strand breaks by Cu<sup>II</sup>-TC-Thio but instead point to a cleavage pattern consistent with single strand breaks. To probe the DNA damage mechanism, cleavage experiments were conducted in the presence of antioxidants and non-covalent DNA priming agents (Figure 4b). Both tiron and *N,N*-dimethylthiourea (DMTU) strongly inhibited DNA cleavage implicating superoxide and peroxide species in the cleavage reaction, respectively. This suggests a linked Cu-superoxo to -peroxo mechanism is chiefly responsible for the oxidative cleavage. A lower degree of inhibition was observed for experiments conducted with *D*-mannitol, *L*-methionine, and sodium azide, indicating a limited role for hydroxyl, hypochlorous, and singlet oxygen radical species, respectively. Overall, the cleavage profiles of Cu<sup>II</sup>-TC-Thio and Cu<sup>II</sup>-TC-1<sup>[9]</sup> are similar, suggesting a conserved reactive oxygen species (ROS) production mechanism dominated by the Cu-triazole character of the complex. Next, the DNA damaging properties of Cu<sup>II</sup>-TC-Thio were examined in the presence of priming agents. Enhanced cleavage was observed upon addition of the major groove binder, methyl green (MG), and the complete inhibition of cleavage upon addition of the minor groove binder, netropsin. Data here indicate that cleavage is occurring primarily from the minor groove, in good agreement with the earlier DNA binding studies. To study the conformational changes associated with DNA damage in more detail, mixtures of pUC19 treated with Cu<sup>II</sup>-TC-Thio were visualised via atomic force microscopy (AFM). In comparison to the untreated control, cleavage of supercoiled DNA is evident from the appearance of DNA fragments in the sample treated with 10 μM Cu<sup>II</sup>-TC-Thio for 30 min (Figure S12). Condensation effects in the treated sample were also clearly visible and distinguished as regions of higher DNA density and vertical topology. Significantly, it appears that after the emergence of sheared DNA, Cu<sup>II</sup>-TC-Thio then condenses portions of fragmented DNA resulting in the formation of discrete compact particles. Such behaviour may explain the condensation observed in MST and CD analyses.

### Cu<sup>II</sup>-TC-Thio mediated DNA damage in PBMCs

DNA lesions formed by Cu<sup>II</sup>-TC-Thio were investigated using a repair-assisted damage detection (RADD) assay.<sup>[18]</sup> Here, DNA from peripheral blood mononuclear cells (PBMCs), isolated from blood samples from individuals with normal blood count were treated with Cu<sup>II</sup>-TC-Thio. The DNA from these cells was then extracted and exposed to different base-excision repair (BER) enzymes, DNA polymerase 1 and a mixture of dNTPs containing a fluorescent dNTP analogue (aminoallyl-dUTP-ATTO-647N). Later, a dye (YOYO-1) was employed to stain DNA and individual DNA molecules were stretched on silanised glass slides. The amount of damage was then quantified based on the incorporation of fluorescent nucleotides—which appear as red dots—per mega base pair of DNA (Figure S13 and S14). Performing the assay with each BER

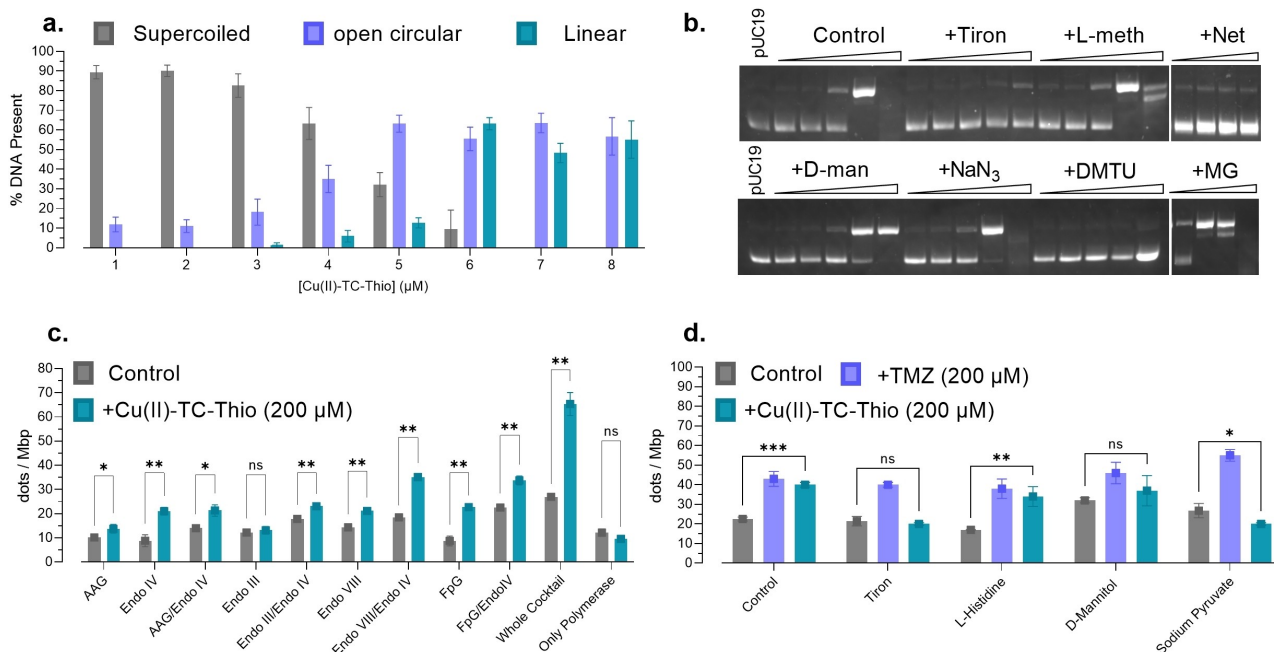


**Figure 4.** DNA oxidation experiments *in vitro* and *in cellulo*. **a.** Dose response of the three DNA forms upon treatment of 400 ng pUC19 with Cu<sup>II</sup>-TC-Thio at various concentrations in the presence of Na-L-ascorbate for 30 minutes. Uncropped versions of these gels are shown in Figure S15. **b.** Cleavage experiments conducted in the presence of ROS scavengers and groove binders. The control experiments, and all scavenger experiments contained 2,4,6,8 and 10 μM Cu<sup>II</sup>-TC-Thio in the presence of 10 mM ROS scavengers, Tiron, L-Methionine (L-Meth), D-mannitol, sodium azide (NaN<sub>3</sub>) and N,N-DimethN,N-Dimethylthiourea (DMTU). Experiments with netropsin (Net, 8 μM) and methyl green (MG 16 μM) contained 4, 6, 8 and 10 μM Cu<sup>II</sup>-TC-Thio. Uncropped gels are shown in Figure S16. **c.** Repair assisted damage detection. Peripheral blood mononuclear cells are isolated from blood samples and treated with tested compound before subjecting to DNA extraction. DNA is extracted and then repaired with a mixture of dNTPs containing a fluorescent dNTP analogue, stained using YOYO-1™ and imaged via fluorescence microscopy. The panel shows DNA lesions observed in samples treated with Cu<sup>II</sup>-TC-Thio using various repair enzyme combinations **d.** Comparison of Cu<sup>II</sup>-TC-Thio and TMZ induction of DNA lesions in the presence of ROS scavengers using whole cocktail repair protocol. The experiments were performed in technical duplicates. Error bars indicate the standard deviation calculated from technical duplicates with significance at  $p < 0.05$  (\*\*\*) represents  $p < 0.001$ , \*\*  $p < 0.01$ , \*  $p < 0.05$ ).

enzyme or combinations thereof provides insight into the type of intracellular lesions induced by the complex. Additionally, since PBMCs are primary non-dividing cells, they are a suitable representative model for probing accurate DNA repair.

In comparison to the untreated control, experiments using the whole BER enzyme cocktail revealed that Cu<sup>II</sup>-TC-Thio (200 μM) increased lesion formation ~4-fold (Figure 4c). Next, to gain insight into the predominant lesion types induced by Cu<sup>II</sup>-TC-Thio, experiments were repeated using single BER enzymes along with combinations thereof. Here, with the exception of Endo III, experiments with Cu<sup>II</sup>-TC-Thio showed increased damage detection from the untreated control samples. Samples exposed to FpG and Endo IV showed the largest responses, with lesion detection increasing by ~2.5 fold. This suggests that significant proportions of oxidised purines such as FapyG and 8-oxoG (repaired by FpG) in addition to abasic sites (recognised by EndoIV)<sup>[9]</sup> are formed. By prophylactically incubating the PBMCs with specific ROS scavengers and repeating the RADD experiment using the whole BER cocktail ROS responsible for intracellular DNA oxidation were identified. Here, experiments conducted in the presence of tiron (O<sub>2</sub><sup>•-</sup>), D-mannitol (<sup>•</sup>OH), L-histidine (<sup>1</sup>O<sub>2</sub>), or sodium

pyruvate (H<sub>2</sub>O<sub>2</sub>) were compared to the untreated control sample and to samples treated with temozolomide (TMZ) in place of Cu<sup>II</sup>-TC-Thio (Figure 4d). Since TMZ is a DNA alkylating agent used to treat glioblastoma multiforme,<sup>[18]</sup> its non-oxidative mechanism provided a critical benchmark and point of comparison for Cu<sup>II</sup>-TC-Thio. Control experiments, conducted without any antioxidant and with equivalent concentrations of both test compounds show Cu<sup>II</sup>-TC-Thio induced a similar degree of DNA damage to TMZ. However, unlike TMZ,<sup>[19]</sup> the efficacy of Cu<sup>II</sup>-TC-Thio is significantly impacted by the presence of antioxidants. Sodium pyruvate, tiron, and D-mannitol all reduced the observed oxidation levels induced by Cu<sup>II</sup>-TC-Thio to baseline while L-methionine showed only a modest impact. Overall, there is good agreement between the intracellular DNA oxidation profiles of Cu<sup>II</sup>-TC-Thio and the earlier *in vitro* experiments with pUC19.

## Conclusion

TC-Thio was rationally designed to demonstrate a method for developing a clinically relevant structural motif of the Tri-Click scaffold with simple chemistry, using commercially

available and inert starting materials. TC-Thio was confirmed to form polynuclear Cu<sup>II</sup> complexes in solution with Cu<sup>II</sup> nitrate as evidenced by ESI-MS. The resulting complex was structurally investigated in silico and found to be a suitable ligand for coordinating both Cu<sup>II</sup> and Cu<sup>I</sup> ions. DNA recognition studies revealed Cu<sup>II</sup>-TC-Thio binds duplex DNA with high affinity, comparable to model polypyridyl and phenanthroline-based systems while also exhibiting a combination of minor groove and phosphate recognition properties. Cu<sup>II</sup>-TC-Thio was found to efficiently mediate oxidative cleavage of plasmid DNA via a superoxide/peroxide-dependent mechanism in a similar fashion to other state-of-the-art multinuclear Cu<sup>II</sup> complexes such as Cu<sub>2</sub>TPNap<sup>[6c]</sup> and Cu<sup>II</sup>-TC-1.<sup>[9]</sup> Further DNA binding analysis via CD, fluorescence melting, and MST using small hairpin DNA sequences (and later AFM imaging of pUC19) revealed Cu<sup>II</sup>-TC-Thio to be an effective DNA condensation agent. DNA cleavage assays were used to gauge the potential application of Cu<sup>II</sup>-TC-Thio as an artificial metallo-nuclease. Here, Cu<sup>II</sup>-TC-Thio was found to be a potent DNA cleavage agent with subsequent experiments showing a superoxide/peroxide dependant mechanism. While it may be the case that these cleavage mechanisms exist independently, it is also possible that Cu<sup>II</sup>-TC-Thio acts as a superoxide dismutase mimetic, converting superoxide to peroxide or Cu-peroxo species which ultimately results in direct damage. *In-cellulo* experiments revealed that Cu<sup>II</sup>-TC-Thio induces a range of oxidative DNA lesions, particularly those recognised by FpG. Additional RADD experiments revealed that Cu<sup>II</sup>-TC-Thio possesses a similar activity profile to the clinically approved temozolomide but with redox environment dependency. Overall, TC-Thio demonstrates the versatility and simplicity of click chemistry in the design of new metallodrugs, paving the way for the development of new clinically relevant and structurally diverse agents using environmentally friendly and cost-effective methodologies. Current efforts on this TC-scaffold are focused on broad spectrum anticancer screening and modification of the scaffold to better understand the structure–activity relationships at play.

### Acknowledgements

This project has received funding from Science Foundation Ireland (12/RC/2275\_P2), the Irish Research Council (IR-CLA/2022/3815), and the Novo Nordisk Foundation (NNF22OC0077099). R. E. F. de P. acknowledges funding from the Government of Ireland Postdoctoral Fellowship program (GOIPD/2021/909). We acknowledge funding from the European Union's Horizon 2020 research and innovation program under the Marie Skłodowska-Curie grant agreement No 861381 (NATURE-ETN). F. W. acknowledges funding from the Swedish Cancer Foundation (201145 PjF) and the Swedish Child Cancer Foundation (PR2019-0037 and PR2022-0014). R. F. and D. T. acknowledge super-computing time at the SFI/Higher Education Authority Irish Center for High-End Computing (ICHEC). Open Access funding provided by IREL.

### Conflict of Interest

The authors declare no conflict of interest.

### Data Availability Statement

The data that support the findings of this study are available in the supplementary material of this article.

**Keywords:** Click Chemistry · Copper · DNA Damage · Nuclease

- [1] A. Radzicka, R. Wolfenden, *Science* **1995**, *267*, 90–93.
- [2] E. S. Henle, S. Linn, *J. Biol. Chem.* **1997**, *272*, 19095–19098.
- [3] F. Mancin, P. Scrimin, P. Tecilla, U. Tonellato, *Chem. Commun.* **2005**, 2540–2548.
- [4] a) Q. Jiang, N. Xiao, P. Shi, Y. Zhu, Z. Guo, *Coord. Chem. Rev.* **2007**, *251*, 1951–1972; b) M. S. Cooke, M. D. Evans, M. Dizdaroglu, J. Lunec, *FASEB J.* **2003**, *17*, 1195–1214.
- [5] a) M. Pitić, G. Pratiel, *Chem. Rev.* **2010**, *110*, 1018–1059; b) A. Kellett, M. O'Connor, M. McCann, M. McNamara, P. Lynch, G. Rosair, V. McKee, B. Creaven, M. Walsh, S. McClean, A. Foltyn, D. O'Shea, O. Howe, M. Devereux, *Dalton Trans.* **2011**, *40*, 1024–1027; c) C. Slator, N. Barron, O. Howe, A. Kellett, *ACS Chem. Biol.* **2016**, *11*, 159–171.
- [6] a) Y. Zhao, J. Zhu, W. He, Z. Yang, Y. Zhu, Y. Li, J. Zhang, Z. Guo, *Chem. Eur. J.* **2006**, *12*, 6621–6629; b) J. W. Chen, X. Y. Wang, Y. Shao, J. H. Zhu, Y. G. Zhu, Y. Z. Li, Q. Xu, Z. J. Guo, *Inorg. Chem.* **2007**, *46*, 3306–3312; c) Z. Molphy, D. Montagner, S. S. Bhat, C. Slator, C. Long, A. Erxleben, A. Kellett, *Nucleic Acids Res.* **2018**, *46*, 9918–9931; d) C. Slator, Z. Molphy, V. McKee, C. Long, T. Brown, A. Kellett, *Nucleic Acids Res.* **2018**, *46*, 2733–2750; e) A. Kellett, M. O'Connor, M. McCann, O. Howe, A. Casey, P. McCarron, K. Kavanagh, M. McNamara, S. Kennedy, D. D. May, P. S. Skell, D. O'Shea, M. Devereux, *MedChemComm* **2011**, *2*, 579–584; f) K. Suntharalingam, D. J. Hunt, A. A. Duarte, A. J. White, D. J. Mann, R. Vilar, *Chem. Eur. J.* **2012**, *18*, 15133–15141; g) C. Lüdtke, S. Sobottka, J. Heinrich, P. Liebing, S. Wedepohl, B. Sarkar, N. Kulak, *Chem. Eur. J.* **2021**, *27*, 3273–3277; h) Z. R. Li, J. Li, W. L. Cai, J. Y. H. Lai, S. M. K. McKinnie, W. P. Zhang, B. S. Moore, W. J. Zhang, P. Y. Qian, *Nat. Chem.* **2019**, *11*, 880–889; i) M. P. Silva, C. Saibert, T. Bortolotto, A. J. Bortoluzzi, G. Schenk, R. A. Peralta, H. Terenzi, A. Neves, *J. Inorg. Biochem.* **2020**, *213*, 111249; j) C. Pereira, G. Farias, F. G. Maranhã, N. Castilho, G. Schenk, B. de Souza, H. Terenzi, A. Neves, R. A. Peralta, *J. Biol. Inorg. Chem.* **2019**, *24*, 675–691; k) R. A. Peralta, A. J. Bortoluzzi, B. de Souza, R. Jovito, F. R. Xavier, R. A. Couto, A. Casellato, F. Nome, A. Dick, L. R. Gahan, G. Schenk, G. R. Hanson, F. C. de Paula, E. C. Pereira-Maia, P. M. S. de, P. C. Severino, C. Pich, T. Bortolotto, H. Terenzi, E. E. Castellano, A. Neves, M. J. Riley, *Inorg. Chem.* **2010**, *49*, 11421–11438.
- [7] H. Struthers, T. L. Mindt, R. Schibli, *Dalton Trans.* **2010**, *39*, 675–696.
- [8] a) T. L. Mindt, H. Struthers, L. Brans, T. Anguelov, C. Schweinsberg, V. Maes, D. Tourwe, R. Schibli, *J. Am. Chem. Soc.* **2006**, *128*, 15096–15097; b) H. Struthers, B. Spingler, T. L. Mindt, R. Schibli, *Chem. Eur. J.* **2008**, *14*, 6173–6183.
- [9] a) N. McStay, C. Slator, V. Singh, A. Gibney, F. Westerlund, A. Kellett, *Nucleic Acids Res.* **2021**, *49*, 10289–10308; b) A. Kellett (DCU), N. McStay (DCU), WO 2023/031375, **2023**.
- [10] Deposition number 2192605 contains the supplementary crystallographic data for this paper. These data are provided

- free of charge by the joint Cambridge Crystallographic Data Centre and Fachinformationszentrum Karlsruhe Access Structures service.
- [11] R. J. Angelici, *Organometallics* **2001**, *20*, 1259–1275.
- [12] a) H. Kargar, M. Ashfaq, M. Fallah-Mehrjardi, R. Behjatmashesh-Ardakani, K. S. Munawar, M. N. Tahir, *J. Mol. Struct.* **2022**, *1253*, 132264; b) T. S. Morais, Y. Jousseume, M. F. M. Piedade, C. Roma-Rodrigues, A. R. Fernandes, F. Marques, M. J. V. de Brito, M. H. Garcia, *Dalton Trans.* **2018**, *47*, 7819–7829.
- [13] Z. Molphy, A. Prisecaru, C. Slator, N. Barron, M. McCann, J. Colleran, D. Chandran, N. Gathergood, A. Kellett, *Inorg. Chem.* **2014**, *53*, 5392–5404.
- [14] a) N. Z. Fantoni, Z. Molphy, S. O'Carroll, G. Menounou, G. Mitrikas, M. G. Krokidis, C. Chatgialiloglu, J. Colleran, A. Banasiak, M. Clynes, S. Roche, S. Kelly, V. McKee, A. Kellett, *Chem. Eur. J.* **2021**, *27*, 971–983; b) A. Prisecaru, Z. Molphy, R. G. Kipping, E. J. Peterson, Y. Qu, A. Kellett, N. P. Farrell, *Nucleic Acids Res.* **2014**, *42*, 13474–13487.
- [15] M. T. Carter, M. Rodriguez, A. J. Bard, *J. Am. Chem. Soc.* **1989**, *111*, 8901–8911.
- [16] M. Jerabek-Willemsen, C. J. Wienken, D. Braun, P. Baaske, S. Duhr, *Assay Drug Dev. Technol.* **2011**, *9*, 342–353.
- [17] N. McStay, A. M. Reilly, N. Gathergood, A. Kellett, *Chem-PlusChem* **2019**, *84*, 38–42.
- [18] A. D. Thomas, *Chem. Res. Toxicol.* **2020**, *33*, 2219–2224.
- [19] Z. D. Nagel, G. J. Kitange, S. K. Gupta, B. A. Joughin, I. A. Chaim, P. Mazzucato, D. A. Lauffenburger, J. N. Sarkaria, L. D. Samson, *Cancer Res.* **2017**, *77*, 198–206.

Manuscript received: April 25, 2023

Accepted manuscript online: June 20, 2023

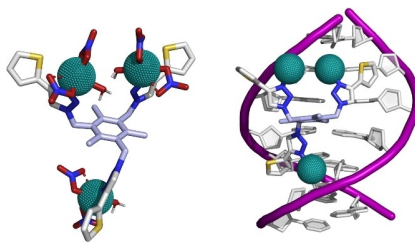
Version of record online: ■■, ■■

## Research Articles

## Artificial Metallonucleases

A. Gibney, R. E. F. de Paiva, V. Singh,  
R. Fox, D. Thompson, J. Hennessy,  
C. Slator, C. J. McKenzie, P. Johansson,  
V. McKee, F. Westerlund,  
A. Kellett\* \_\_\_\_\_ e202305759

A Click Chemistry-Based Artificial Metallo-  
Nuclease



Click chemistry was used to prepare TC-Thio, a new artificial metallo-nuclease. TC-Thio coordinates up to three  $\text{Cu}^{\text{II}}$  ions and is a potent DNA damaging agent that binds and cleaves from the minor groove. Activity was assessed in primary human cells using single molecule imaging of DNA.